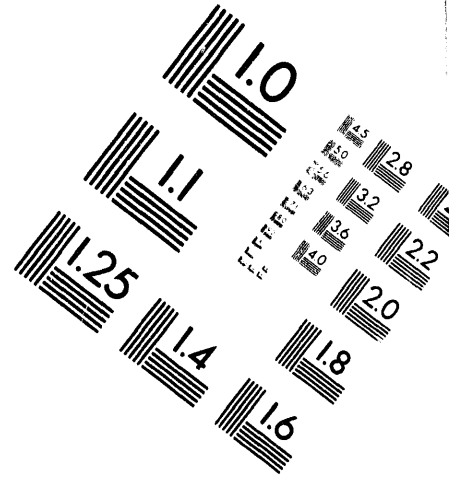
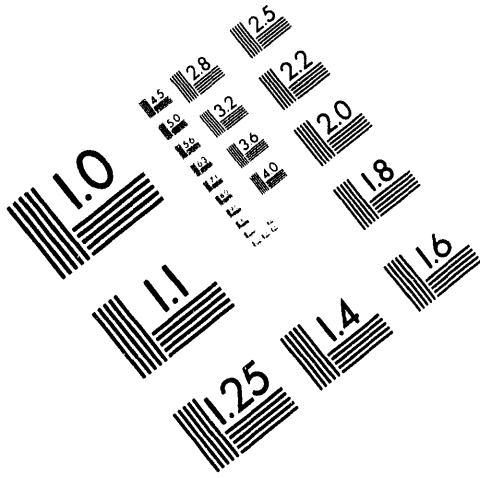




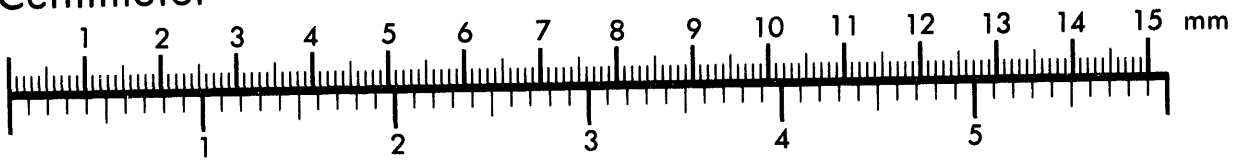
**AIM**

**Association for Information and Image Management**

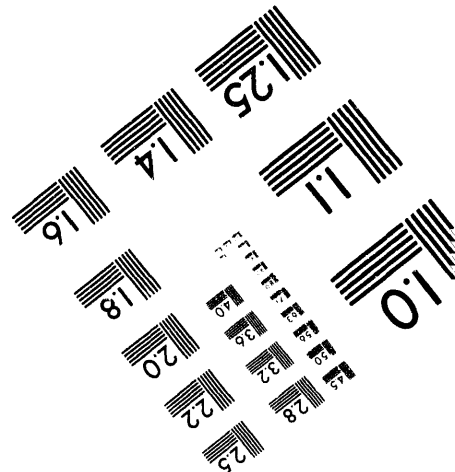
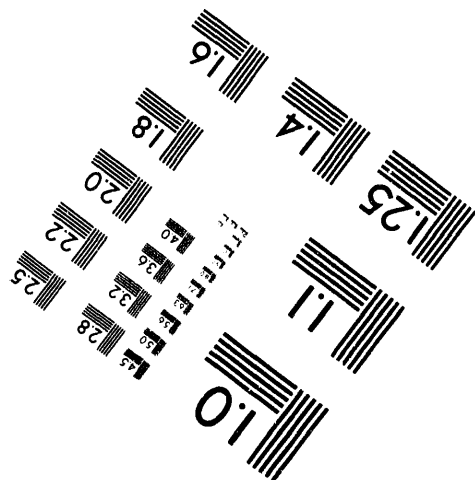
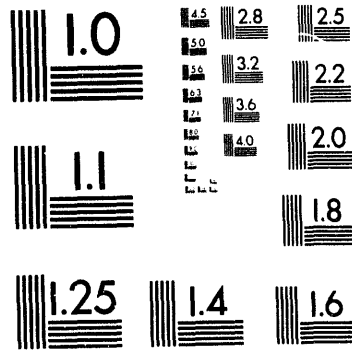
1100 Wayne Avenue, Suite 1100  
Silver Spring, Maryland 20910  
301/587-8202



Centimeter



Inches



MANUFACTURED TO AIM STANDARDS  
BY APPLIED IMAGE, INC.

**1 of 1**

LA-UR-94- 2784

Title: NONLINEAR BEAM EXPANDER FOR ESNT

Author(s): Daniel P. Rusthoi  
Barbara Blind  
Robert W. Garnett  
David S. Hanna  
Andrew J. Jason  
Robert H. Kraus, Jr.  
Filippo Neri

Submitted to: 17th International Linac Conference  
KEK National Laboratory for High Energy Physics  
1-1 Oho, Tsukuba, Ibaraki, 305, Japan  
August 21-26, 1994

DISCLAIMER

This report was prepared as an account of work sponsored by an agency of the United States Government. Neither the United States Government nor any agency thereof, nor any of their employees, makes any warranty, express or implied, or assumes any legal liability or responsibility for the accuracy, completeness, or usefulness of any information, apparatus, product, or process disclosed, or represents that its use would not infringe privately owned rights. Reference herein to any specific commercial product, process, or service by trade name, trademark, manufacturer, or otherwise does not necessarily constitute or imply its endorsement, recommendation, or favoring by the United States Government or any agency thereof. The views and opinions of authors expressed herein do not necessarily state or reflect those of the United States Government or any agency thereof.

MASTER



Los Alamos  
NATIONAL LABORATORY

Los Alamos National Laboratory, an affirmative action/equal opportunity employer, is operated by the University of California for the U.S. Department of Energy under contract W-7405-ENG-36. By acceptance of this article, the publisher recognizes that the U.S. Government retains a nonexclusive, royalty-free license to publish or reproduce the published form of this contribution, or to allow others to do so, for U.S. Government purposes. The Los Alamos National Laboratory requests that the publisher identify this article as work performed under the auspices of the U.S. Department of Energy.

# NONLINEAR BEAM EXPANDER FOR ESNIT<sup>1</sup>

D. Rusthoi, B. Blind, R. Garnett, D. Hanna, A. J. Jason, R. H. Kraus, Jr., F. Neri  
Los Alamos National Laboratory, Los Alamos, NM 87545 USA

## ABSTRACT

We describe the design of a beam-redistribution and expansion system for the Japanese Atomic Energy Research Institute (JAERI) Energy Selective Neutron Irradiation Test Facility (ESNIT). The system tailors the beam exiting a deuteron accelerator at energies from 20 to 35 MeV for deposition on a lithium neutron-production target. A uniform beam-intensity distribution in a well-defined irradiation area is required at the target and is achieved by the use of nonlinear elements. The design of the high-energy beam transport (HEBT) for ESNIT includes a 90° achromatic bend, a matching section with an energy-compacting cavity, a nonlinear beam expander, a target imager, a shielding dipole, and an rf-cavity system to add energy spread to the beam before it impinges on the target. The system meets performance requirements at multiple energies and currents, and for different spot sizes on target.

## INTRODUCTION

The JAERI ESNIT facility will use a cw (continuous wave) 175-MHz deuteron accelerator to perform research on fusion-reactor materials in a high-energy neutron field by obtaining materials-irradiation data up to the primary operating regime of 35–40 MeV where the 14-MeV fusion-neutron spectrum is approximated when deuterons produce neutrons in a lithium target. A nonlinear beam expander and an energy-dispersing cavity are required to provide uniform energy deposition in the target volume.

## DESIGN REQUIREMENTS / GOALS

The nonlinear beam expander must operate at multiple energies (10–40 MeV) and currents (up to 100 mA) as well as produce a uniform spot size of 7 cm x 7 cm and a beam energy spread of  $\pm 0.5$  MeV on target. The design goal also includes the capability of varying the energy spread and spot size on target.

## DESIGN DESCRIPTION

The ESNIT HEBT consists of: (1) a five-cell 90° periodic achromatic bend, (2) a four-quadrupole matching section with an energy-compacting cavity, (3) a nonlinear beam expander, (4) a five-quadrupole imager, (5) a 7.5° shielding dipole, and (6) an energy-dispersing cavity. Following the last cavity, there is a 4-meter drift to the target that allows room for the placement of shielding components. The ESNIT HEBT components are described below and are shown in Fig. 1.

**Achromat.** The 90° achromatic bend is included in the HEBT for compatibility with a proposed Grumman layout for IFMIF (International Fusion Materials Irradiation Facility)<sup>2</sup>. The achromat has five cells with two 9° dipoles per cell and an F-D structure that is compatible with the F-D structure in the linac. At all energies, the zero-current phase advance is 72° per cell.

**Matching Section.** The matching-section magnets are tuned to assure the proper input beam to the expander section. The matching section also includes an rf cavity that reduces the beam-energy spread to improve the performance of the HEBT.

**Nonlinear Beam Expander.** The nonlinear beam expander<sup>3</sup> consists of two octupoles separated by two quadrupoles. The beam edges are folded into the core in vertical phase space by the first octupole, and in horizontal phase space by the second octupole to produce a well-defined and closely uniform distribution on target. The two octupoles have comparable pole-tip fields (~0.6 T).

**Beam Imager.** The beam imager consists of five quadrupole magnets that focus the beam to nearly coincident waists upstream of the shielding dipole and the energy-dispersing cavity. This allows the dipole and cavity to have reasonable apertures. The imager also serves to size the beam on target. The first four magnets are sufficient to size the beam and to produce (to first-order) the waists. However, because of the folding, the beam is not smallest at the first-order waists; so the last quadrupole is needed to control the tails of the folded beam to produce the smallest-size beam entering the cavity.

**Shielding Dipole.** A 7.5° bend is used to shield most of the HEBT from the backstreaming neutrons produced at the target. Shielding in and around the beam waists at the energy-dispersing cavity and a backstreaming-neutron dump (placed upstream of the 7.5° bend and out of the beamline) protect most of the HEBT elements from radiation exposure. The bend angle was chosen as a compromise to maximize the separation between the beamline and backstreaming neutrons while minimizing the dispersion effects at the target.

**Energy-Dispersing Cavity.** The last element is an rf cavity used to control the longitudinal energy deposition in the target by increasing energy spread, thereby spreading the Bragg peak throughout the target depth.

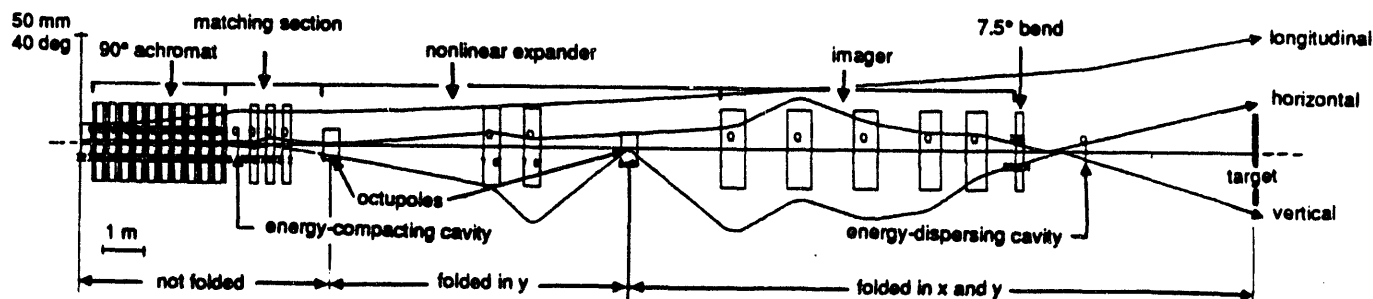


Fig. 1: A schematic of the ESNIT HEBT calculated with TRACE-3D, showing rms beam envelopes at 35 MeV and 100 mA. (The nonlinear elements produce negligible effect at the rms extent.)

## INPUT BEAM TO HEBT

The input beam used to simulate the HEBT was the 10,000-particle output distribution of a PARMILA run for a superconducting IFMIF linac. The parameters of the beam at 35 MeV, given in the middle of the last quadrupole of the linac (a D-quad), are shown in Table I. At 20 MeV, the transverse lab emittances increase by 33%. With the remaining half D-quad and a 24.5-cm drift, the beam is extremely well matched into the achromatic bend.

Table I: Input Beam (rms, unnormalized, 35 MeV)

(Units: mm, mrad, keV, deg)		
$\alpha_x=0$	$\alpha_y=0$	$\alpha_z=0$
$\beta_x=0.3845$	$\beta_y=1.4192$	$\beta_z=0.1496$
$\epsilon_x=1.05\pi$	$\epsilon_y=1.05\pi$	$\epsilon_z=300\pi$

## PERFORMANCE AND SIMULATIONS

To simulate the ESNIT HEBT, we used the code PARMILA with the 10,000-particle distribution mentioned above. TRACE-3D and MARYLIE were both used for the design and fitting of the matching-section quadrupoles. Figures 2-5 show the beam-particle distributions on target in  $x, y$  space as well as horizontal and vertical profiles depicting the flatness of the distributions. The nominal tune has been achieved and is shown in Fig. 2. In Fig. 3, the current has been decreased from 100 mA to 50 mA with no adjustment of beamline elements. The flatness of the distribution is essentially maintained and appears to be insensitive to beam-current variations.

Comparing Figs. 2 and 4, one can see the difference in the distribution on target when there is a change in the beam energy from 35 MeV to 20 MeV. In this instance, all magnets are scaled by beam rigidity followed by optimization of the matching section. Although no simulations were performed outside of the 20-35 MeV range, it is clear the design is not limited to this range.

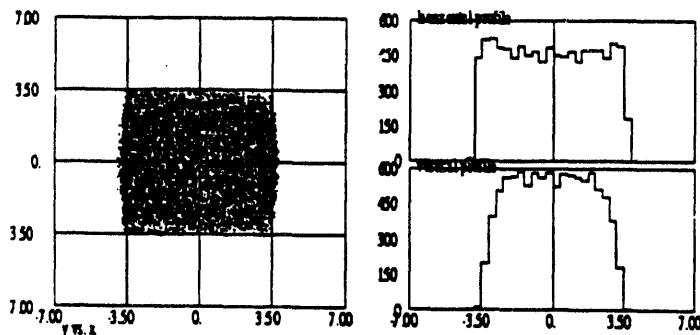


Fig. 2: 35 MeV, 100 mA, 7 cm x 7 cm,  $\pm 0.5$  MeV

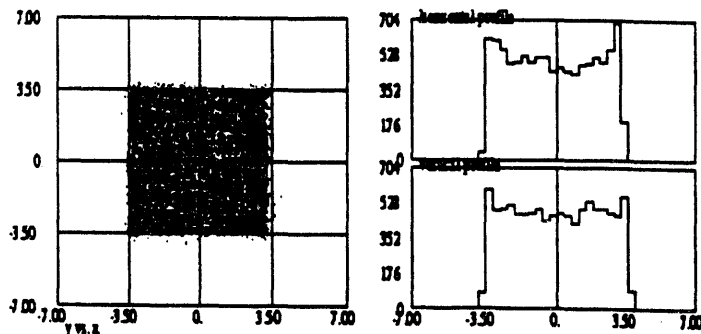


Fig. 3: 35 MeV, 50 mA, 7 cm x 7 cm,  $\pm 0.5$  MeV

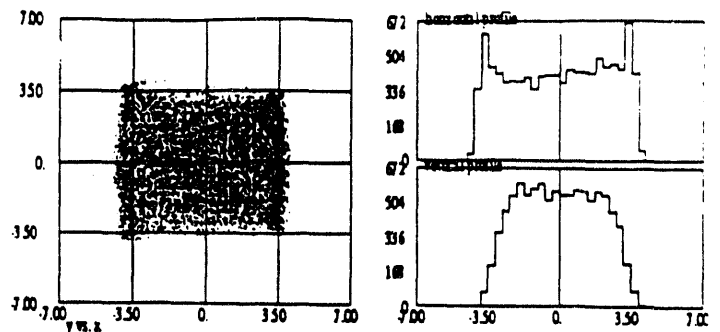


Fig. 4: 20 MeV, 100 mA, 7 cm x 7 cm,  $\pm 0.5$  MeV

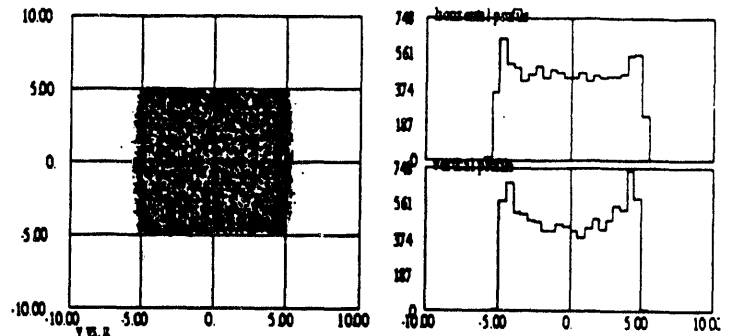


Fig. 5: 35 MeV, 100 mA, 10 cm x 10 cm,  $\pm 0.5$  MeV

Finally, Figs. 2 and 5 illustrate the effect on the distribution uniformity when using the imager alone to adjust the spot size on target. Spot sizes of 5 cm x 5 cm, 7 cm x 7 cm, and 10 cm x 10 cm with uniform distribution were created on target.

**Energy-Spread Variations.** The final rf cavity increases the energy spread from  $\pm 0.25$  MeV to  $\pm 0.5$  MeV. It also produces a relatively flat distribution in energy spread in the  $x$ -plane (see Fig. 6a). The distribution exhibits a sharp peak on one end, resulting from a peak in the phase distribution of the beam out of the linac (which could be rephased). Figure 6b shows that the horizontal position is not correlated with the energy.

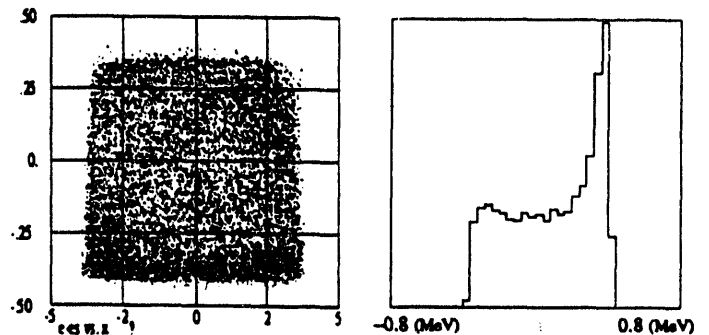


Fig. 6a:  $\Delta E$  (MeV) vs.  $x$  (cm) Fig. 6b:  $\Delta E$  profile

## APERTURE REQUIREMENTS

Beamline aperture is of concern because of the limitations in achieving the required field strength from large aperture multipole magnets. The beam is large in one plane in each octupole, and can get very large in the imager section depending on the beam spot size at the target. Figure 7 shows the beam envelope from the PARMILA simulation for 100%

of the beam through the HEBT, starting with the matching section, for the nominal case of a 100-mA, 35-MeV beam tuned to produce a uniform 7 cm x 7 cm distribution at the target. The maximum extent of the simulated beam in the first and second octupoles is 11 mm (in  $y$ ) and 25 mm (in  $x$ ), respectively. The beam envelope is largest inside the imager quadrupoles immediately following the second octupole, scaling with the final beam spot size on target. Producing a 10 cm x 10 cm spot size on target increases the maximum beam envelope in these quadrupoles to approximately 50 mm.

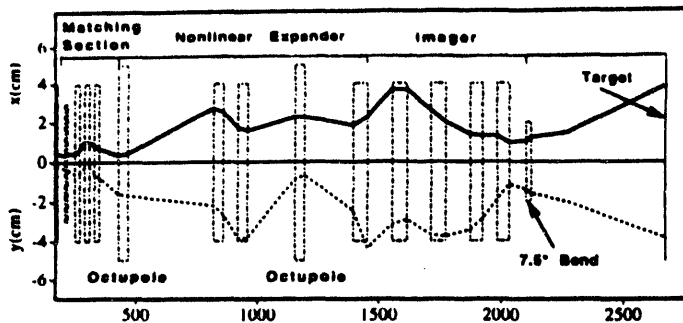


Fig. 7: Total beam size (cm) vs. HEBT position (cm) (In contrast to Fig. 1, nonlinearities are evident.)

### TUNING THE HEBT

At the entrances to the octupoles in the expander, the beam quantities of interest are the transverse rms-beam sizes, divergences, and their ratios. The ratios govern the size of the beam spot at the target, while the rms dimensions (size and divergence) govern the distribution on target.

The nominal input beam desired at the entrance to the first octupole of the expander is given in Table II.

Table II: Nominal Beam to Expander (rms, 35 MeV)

$x=0.784$ mm	$y=4.495$ mm
$x'=1.440$ mrad	$y'=3.141$ mrad
$r_{12}=-0.3680$	$r_{34}=+0.9972$

To adjust the HEBT to operate at different energies, all magnets are initially scaled according to beam rigidity. Beams of different energies, however, have different transverse lab emittances; if the matching-section magnets were scaled only according to beam rigidity, the beam rms dimensions would be larger for lower-energy beams (larger emittances) and smaller for higher-energy beams (smaller emittances). Although this would not affect the spot size on target, the lower-energy beam would be folded by the octupoles at more populated points in the distribution, resulting in a distribution on target with spikes around the edges of the beam spot. Correspondingly, the higher-energy beam would be folded at less populated regions and would have a peaked center on target. In addition to differences in the transverse emittances, the matching section corrects for different Twiss parameters out of the accelerator and different space-charge forces upstream of the nonlinear expander when such forces are significant.

Beams of different energies may have different initial distributions. For different initial distributions with the same rms dimensions, the spot size on target will be the same, but the distribution at the target will be different. In these cases,

the rms dimensions at the octupoles for each transverse plane must be scaled by a fixed factor to achieve a more favorable distribution, while preserving the rms-size-to-divergence ratios. If the beam on target is too peaked in the center, the rms dimensions at the octupoles are too small and should be increased. Similarly, if the beam has spikes at the edges of the distribution, the rms dimensions are too large and should be decreased.

Diagnostics must be available to characterize the input beam into the expander and the beam distribution on target. To obtain adequate uniformity, adjustments to the matching-section quadrupoles may be necessary as mentioned above. In tuning the matching-section quadrupoles, guidance from a beam-optics code such as TRACE-3D is useful. After the beam distribution on target is made acceptably uniform, the size of the distribution is adjusted using the first four imager quadrupoles, again using a code such as TRACE-3D. Several iterations of the procedure may be necessary to obtain a beam with both the right size and distribution.

### SPACE-CHARGE EFFECTS

The effects of the space-charge forces acting on the beam distribution must be compensated for in any expander design. These forces are beam-current dependent and nonlinear. These forces are also largest when the beam is brought to a waist, such as at the center of each octupole. It is therefore more difficult to "fold" the tails of a high-current beam (than a low-current beam), resulting in an  $x,y$  distribution on target that is not exactly rectangular, even though nearly uniform in intensity. For lower average beam currents, the beam will be more rectangular but slightly less uniform for the same magnet settings (due to differing beam distributions at the expander). This effect can be seen by comparing Figs. 2 and 3, showing the results of the 100-mA and 50-mA beam simulations.

During accelerator turn-on and tune-up, it may be necessary to operate at lower beam currents. To optimize the uniformity of the beam on target for various beam currents, it will be necessary to tune the matching section in order to compensate for different degrees of space charge and the slightly shifting position of each beam waist. However, if variations in the uniformity of the beam on the target are small over the range of beam currents desired and the power density on target remains within tolerable limits, it should be possible to operate the expander at the full-current magnet settings even during turn-on and tune-up of the accelerator.

### HIGH-ORDER EFFECTS

Duodecapoles, which can be added for halo control, were used, even though their effect could not be seen in the PARMILA simulations of the ESNIT expander. This is because of the limitations of a 10,000-particle simulation from which no beam is visible outside of a  $3\sigma$  distribution. Actual beams likely have halo particles at  $5\sigma$  that can be contained by octupoles with appropriate duodecapole components.

### REFERENCES

- Work supported and funded by the Japanese Atomic Energy Research Institute under the auspices of the US Dept of Energy
- "Deuteron Linac Design Studies for ESNIT/IFMIF", R. A. Jameson, et. al., LA-CP-94-136, Los Alamos Nat'l Lab. Report, June 1994
- B. Blind, "Production of uniform and well-confined beams by nonlinear optics", Nucl. Instrum. Meth., B56/57 (1991)

**DATE  
FILMED**

**10/19/94**

**END**

